Sensors and Actuators B 180 (2013) 35–42

Contents lists available at SciVerse ScienceDirect

Sensors and Actuators B: Chemical

journal homepage: www.elsevier.com/locate/snb

Integration of organic opto-electrowetting and poly(ethylene) glycol diacrylate (PEGDA) microfluidics for droplets manipulation

Tung-Ming Yu[a,*], Shih-Mo Yang[a], Chien-Yu Fu[c], Ming-Huei Liu[d], Long Hsu[a], Hwan-You Chang[c], Cheng-Hsien Liu[b,*]

[a] Department of Electrophysics, National Chiao-Tung University, No. 1001, University Road, Hsinchu, 300, Taiwan, ROC
[b] Department of Power Mechanical Engineering, National Tsing-Hua University, No. 101, Section 2, Kuang-Fu Road, Hsinchu, 30013, Taiwan, ROC
[c] Institute of molecular medicine, National Tsing Hua University, No. 101, Section 2, Kuang-Fu Road, Hsinchu, 30013, Taiwan, ROC
[d] Sinonar Corp., No. 8, Section 1, Prosperity Road, Hsinchu Science Park, Hsinchu, 30078, Taiwan, ROC

ARTICLE INFO

Article history:
Received 31 August 2011
Received in revised form
11 December 2011
Accepted 19 December 2011
Available online 26 December 2011

Keywords:
Opto-electrowetting (OEW)
TiOPc
Photo-conductor
Electrowetting on dielectric (EWOD)
Dielectrophoresis (DEP)
Poly(ethylene) glycol diacrylate (PEGDA)

ABSTRACT

This paper reports a fabrication technology which integrates organic opto-electrowetting (OEW) with PEGDA-based microfluidics between stacked ITO glass chips for droplets generation and manipulation. Organic OEW can be realized by using titanium oxide phthalocyanine (TiOPc) as a photoconductive layer. Optical images can be projected on an organic OEW area to induce the local virtual electrodes which reduce the surface energy for actuating droplets. Low-molecular-weight (LMW) PEGDA (poly(ethylene) glycol diacrylate) material is used to form stable and biocompatible microchannels between the stacked ITO glass chips by UV photopolymerization process. PEGDA-based microfluidics provides a simpler way to enhance droplets applications in organic OEW. We demonstrate (1) the droplet formation in PEGDA microstructure, (2) the motion of droplet-in-air and droplet-in-oil operated by TiOPc OEW in this platform. This technology requires only spin-coating and UV exposure and is more cost-effective than previous methods.

1. Introduction

Droplet-based systems have been mainly studied in the well calibrated droplet formation and the droplet manipulation in microfluidics [1]. Different approaches of droplet formation can produce many kinds of droplets, such as liquid and oil droplets, for material science and biochemical applications. T-junctions and flow-focus microstructures have been comprehensively designed for droplet formation and fabricated by silicon etching or soft lithography process [2–6]. Electrowetting (EW) and dielectrophoresis (DEP) can provide droplet manipulation on the electrode-patterned substrate for lab-on-a-chip applications. Electrowetting technology has accomplished several fluidic functions in handling and actuating droplets, such as droplet transportation, mixing, and separation [7–11]. Electrical control without moving parts has advantages over traditional mechanical control with pumps and valves, which may cause mechanical issues, such as structural failing, clogging, leaking and unwanted mixing among different chemical reagents. DEP utilizes the liquid electrical properties and non-uniform electrical field distribution to actuate either non-conductive or dielectric droplets [12]. In recent years, the advanced technologies like opto-electrowetting (OEW) and optoelectronic tweezers (OET) have been developed to produce light-induced electrowetting and DEP forces for droplets manipulation [13–19]. Wu's group firstly demonstrated OEW by integrating amorphous silicon (a-Si) as a photoconductor into electrowetting on dielectrics (EWOD) devices [14]. By projecting optical images to alternate conductivity of the photoconductor layer, virtual electrodes can be formed to induce OEW and may replace the complex physical electrodes required for complicated signal control in electrowetting systems. In this study, we focus on integrating droplets formation and OEW with a new and cost-effective fabrication process suitable for biological applications. Two technologies, TiOPc-based OEW and PEGDA-based microfluidic chip, are implemented for this purpose. The TiOPc organic photoconductor provides an alternative for OEW applications because of its many advantages, including non-toxicity, low cost, easy coating process, flexibility, and high photosensitivity [20–23]. In previous microfluidic chips for droplet formation, silicon etching, photolithography and polydimethylsiloxane (PDMS) molding processes are the common fabrication methods. In the a-Si based optoelectronic tweezers (OET) systems [24–30], the SU-8 microstructure is patterned on the ITO glass and adhered to the

* Corresponding author. Tel.: +886 3 5715131x33706.
E-mail addresses: ark.ep96g@g2.nctu.edu.tw (T.-M. Yu), liuch@pme.nthu.edu.tw (C.-H. Liu).

0925-4005/$ – see front matter © 2011 Elsevier B.V. All rights reserved.
doi:10.1016/j.snb.2011.12.059

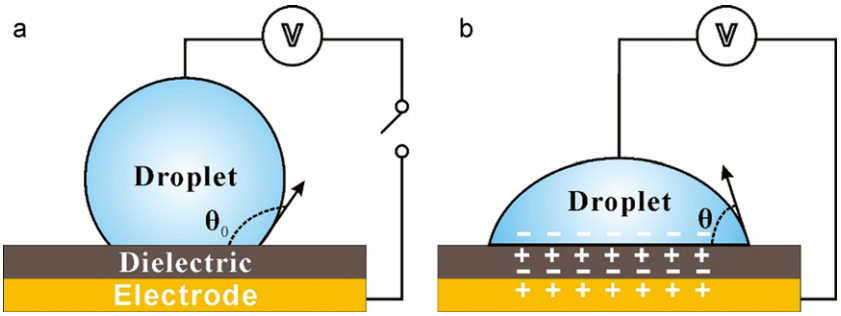

Fig. 1. Contact angle changed by EWOD effect. (a) A droplet rests on the hydrophobic surface above a dielectric layer without an applied voltage. (b) The contact angle between a droplet and a dielectric layer reduces when a voltage is applied across them.

a-Si coated ITO glass by using a UV-curable epoxy [30]. However, these methods are not suitable for TiOPc OEW between the stacked ITO glasses. A series of steps in lithography and UV-curable epoxy adhesion increase the complexity of the fabrication and the etching process may damage the coating of organic TiOPc material. We demonstrated PEGDA-based microfluidic structure made by using the UV photopolymerization. This method provides a solution for integrating TiOPc-based OEW with droplets formation in a single chip. PEGDA is widely used in biological fields because of its biocompatible property and convenient fabrication [31–36]. Hwang et al. reported a new method for the fabrication of PDMS microstructure by using micropatterned LMW PEGDA (MW 258) master molds [37]. The mold of LMW PEGDA has a stable and robust structure and its thickness is defined by commonly available spacer materials (tapes). We combine the advantages of TiOPc OEW and LMW PEGDA mold technologies to achieve a simpler process for embedding TiOPc OEW into the PEGDA-based microfluidic structure. The fabrication of PEGDA microstructure eliminates the need of SU-8 etching and UV-curable epoxy steps in the optoelectronic systems. The thickness of PEGDA microstructure can be defined by tapes, which eliminate the rotation rate test of SU-8 spin-coating for finding the optimal thickness parameters. This rapid fabrication method provides more possibilities in the applications of droplets in digital microfluidics.

2. Theory

EWOD is a technology of utilizing the electrical potential to change surface energy for modulating contact angles between liquid and insulator (dielectric layer) interfaces. Fig. 1(a) shows a polarizable and conductive liquid droplet is initially rested on a hydrophobic surface of a dielectric layer. When an electrical potential is applied between the droplet and the dielectric layer to produce redistribution of charges within the interface of droplet and the dielectric layer, the surface of dielectric layer become wet to reduce the droplet's contact angle (showed in Fig. 1(b)). The hydrophilized surface is a result of lowering the energy of liquid–solid interface in the droplet-insulator-electrode system. The following equation describes the relationship between the contact angle and the applied voltage:

$$\cos\theta(V) = \cos\theta_0 + \frac{\varepsilon\varepsilon_0}{2\gamma_{LV}d}V^2 \quad (1)$$

where $\theta(V)$ is the contact angle when a potential is applied, θ_0 is the contact angle without applied potential, ε is the dielectric constant of the dielectric layer, ε_0 is the dielectric constant of vacuum, γ_{LV} is the surface tension at the liquid–vapor interface, d is the thickness of the dielectric layer, and V is the applied voltage.

According to the definition of Eq. (1), the contact angle is affected by the voltage applied on the liquid–insulator structure, the dielectric constant and thickness of the dielectric layer. OEW integrates photoconductive material into an EWOD device to form a light-controlled impedance layer between the dielectric layer and electrode. Without light illumination, the high impedance property of the photoconductive TiOPc layer results in very little voltage drops across the insulator (SU-8) and the contact angle remains the same as without electrowetting effect (Fig. 2(a)). When light illuminates on the TiOPc OEW device, the conductivity of the TiOPc layer increases by several orders of magnitude due to the electron–hole pair generation (Fig. 2(b)). Because the impedance of TiOPc layer is reduced with light illumination, most of the voltage drops across the SU-8 layer occur at the illuminated region to decrease the contact angle. The virtual electrodes induced by optical images generate electrowetting effect to manipulate droplets with AC bias. Fig. 2(c) is the equivalent circuit model of the TiOPc OEW device. R_{TiOPc} and C_{TiOPc} are the lumped resistance and capacitance of TiOPc, C_{SU-8} is the lumped capacitance of SU-8, and R_{water} and C_{water} are the lumped resistance and capacitance of the water layer, respectively. By adjusting the frequency of the electrical potential across C_{TiOPc}, C_{SU-8} and C_{water}, the impedances of SU-8 and TiOPc layer are controlled for the OEW actuation. The large impedance of SU-8 layer and the high light conductivity of TiOPc result in most of the voltage drop across the SU-8 layer to generate the EOW force on the droplets with light illumination. When no light is emitted on the TiOPc OEW device, the low dark conductivity of TiOPc layer results in the less voltage drop across the SU-8 layer which cannot produces the enough OEW force to manipulate droplets.

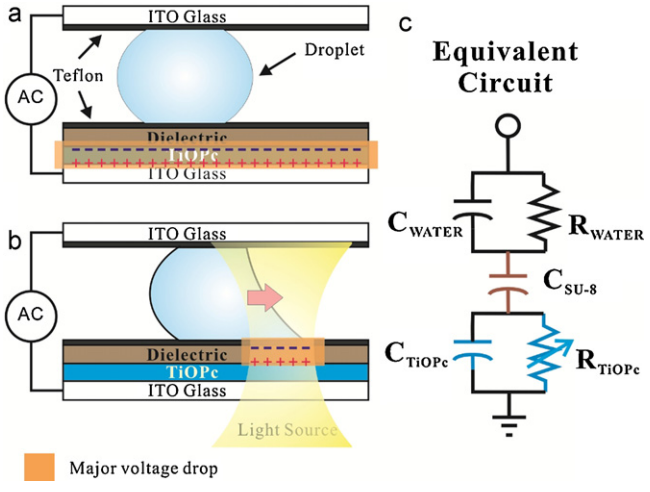

Fig. 2. Principle of TiOPc OEW. (a) Voltage drop is distributed evenly over the TiOPc layer without light illumination. (b) Most voltage drop occurs on the local area of the SU-8 layer illuminated by light source. (c) The equivalent circuit model of our TiOPC OEW device.

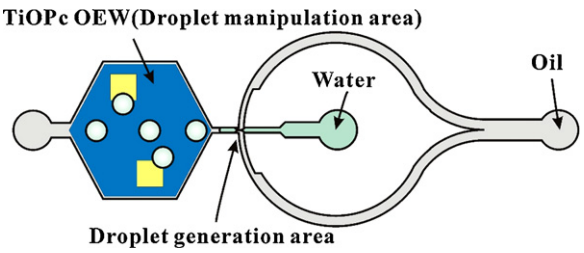

Fig. 3. The working principle of TiOPc OEW in PEGDA microfluidic chip. Oil and water meet at the droplet generation area for producing well calibrated droplets. TiOPc OEW provides the driving force on droplets in the droplet manipulation area.

3. Methods

3.1. Device working principle

Our TiOPc OEW in the PEGDA microfluidic chip includes two areas, which are the droplet generation area and the droplet manipulation area, as illustrated in Fig. 3. In this system, oil and water, which are respectively defined as the continuous phase and the dispersed phase, are pumped into microchannels to enable the mechanism of droplet formation. Two phase flows meet in the droplet generation area, which utilizes the flow-focus channel junction of the oil and water streams to produce monodispersed droplets. After entering the droplet manipulation area (TiOPC OEW), water droplets are controlled by dynamically light-induced electrowetting.

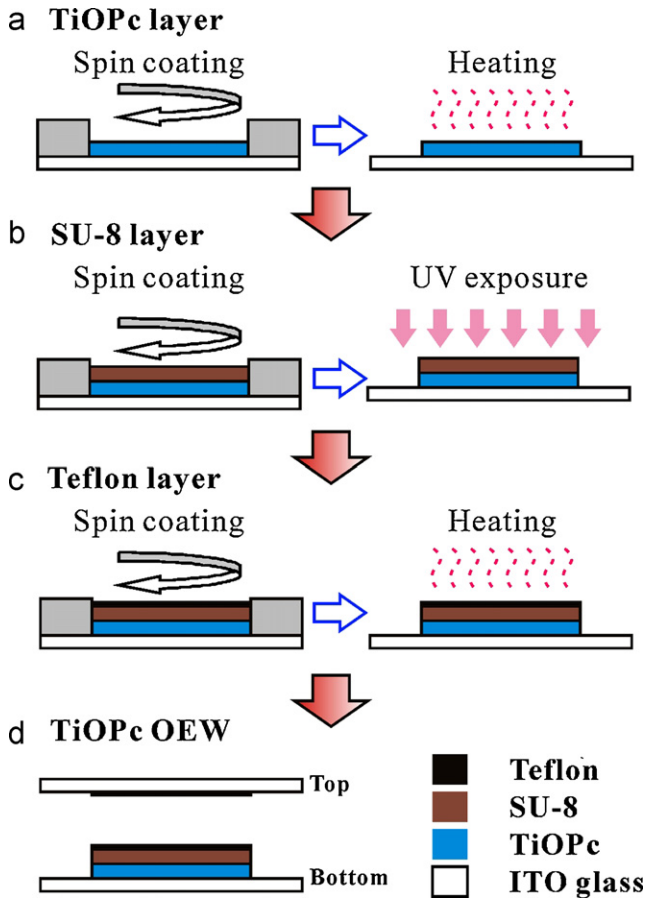

Fig. 4. The fabrication of TiOPc-based OEW device. (a) TiOPc spin-coating on a bottom ITO class. (b) Dielectric layer (SU-8) spin-coating and UV exposure. (c) Teflon spin-coating for increasing the hydrophobic property of the SU-8 surface. (d) The structure of TiOPc-based OEW device.

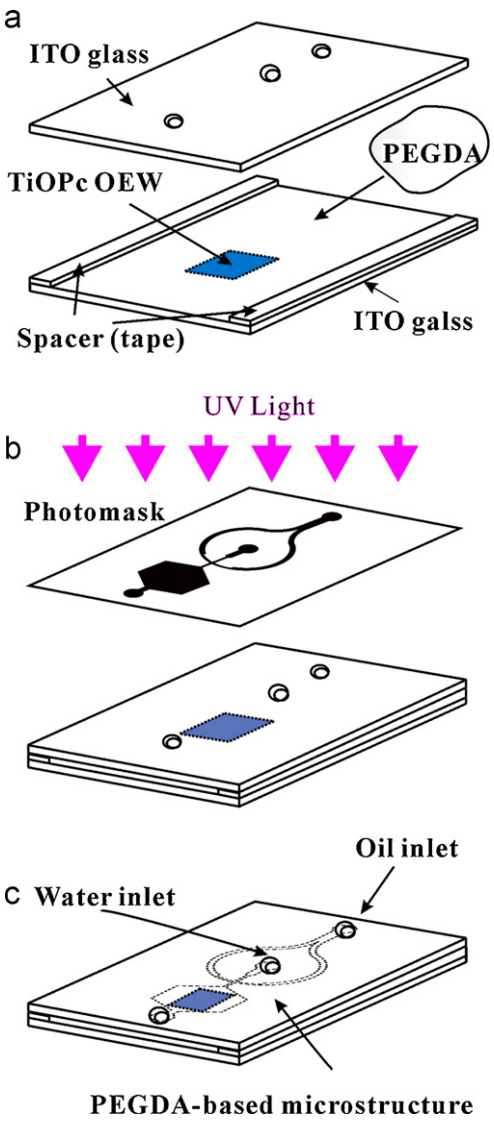

Fig. 5. PEGDA-based microfluidic structure fabrication steps. (a) PEGDA photocurable solution is loaded into the stacked ITO glass chips from inlets. (b) PEGDA photopolymerization process begins by UV light after the photomask is aligned to TiOPc-coated surface, inlet holes and outlet holes. (c) Photocurable PEGDA-based microfluidic structure is constructed after ethanol washing.

3.2. Organic opto-electrowetting fabrication

The working principle of the organic OEW is demonstrated in Fig. 2. TiOPc, SU-8 (dielectric layer) and Teflon, from bottom to top, are spin-coated on the bottom ITO glass with the thicknesses about 1 μm, 1 μm, and 20 nm, respectively. The flowcharts of organic OEW fabrication are shown in Fig. 4. TiOPc is spin-coated on the bottom ITO glass and put on the hot plate at 120 °C for 30 min to enhance TiOPc adhesion with the ITO glass (Fig. 4(a)). SU-8 is spin-coated on TiOPc layer as the dielectric layer and exposed by UV photopolymerization (Fig. 4(b)). Teflon film is spin-coated on SU-8 layer and heated at 150 °C overnight to increase the hydrophobic property of the surface (Fig. 4(c)). Top ITO glass has two inlets and one outlet, and is spin-coated with 20 nm of Teflon. Fig. 4(d) shows the combination of the top and bottom chips to construct TiOPc-based OEW device. All steps of the organic OEW fabrication are accomplished by operating the spin-coating and UV exposure machines in the laboratory. Comparing to the a-Si based OEW device fabricated by using plasma enhanced chemical vapor deposition (PECVD) in the foundry, our fabrication method offers a

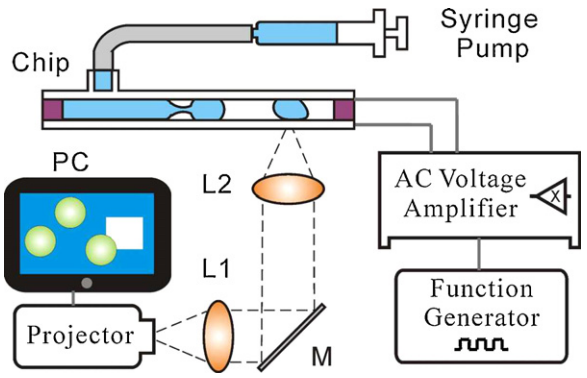

Fig. 6. Set-up of the optical, electrical and pumping parts in the system. The dynamic light pattern is projected onto the operation region within the TiOPc OEW area. Liquid droplets are generated via PEGDA-based microchannels. A function generator and AC voltage amplifier are utilized to provide external AC voltage for EWOD driving power.

simpler and cost-effective approach to develop OEW applications in the laboratory.

3.3. PEGDA-based microfluidics fabrication

The method of fabricating PEGDA-based microfluidic structure is shown in Fig. 5. The photocurable monomer solution is prepared by mixing 1 mL of PEGDA (MW 258 Da, 99%) with 20 μL of DMPA (10 wt%) photoinitiator and then loaded into the space of two parallel ITO glass chips with a 40 μm tape in between, as shown in Fig. 5(a). PEGDA and 2,2-dimethoxy-2-phenyl-acetophenone (DMPA) are provided by Sigma–Aldrich (Wisconsin, USA). Fig. 5(b) shows UV photopolymerization of PEGDA by using a photomask to pattern the microfluidic structure. Finally, a PEGDA-based microfluidic structure, as shown in Fig. 5(c), is constructed by ethanol washing of unexposed PEGDA through inlets.

3.4. Experiment system setup

The experimental system includes three parts, which are the optical part, electrical part and pump part, as shown in Fig. 6:

(1) **Optical part** generates programmable optical images on the TiOPc OEW area to control the conductivity of TiOPc and induce virtual electrodes. This part includes a projector, an optical lens module, a microscope and a CCD camera. The optical lens module is integrated with a condensing lens L1, a 10× objective lens L2 and a mirror M. L1 collimates the optical image generated by the projector. The mirror M is a broadband dielectric mirror which allows the reflection of light wavelengths from 650 to 1200 nm suitable for optical absorption of TiOPc. L2 transfers the collimated optical images to the focus plane of the OEW chip. The optical images produced from the projector with Microsoft PowerPoint on a PC are transmitted though the optical lens module into the OEW device. The image of the microscope is captured by the CCD. When a AC voltage is applied across the OEW device, the electric fields become higher at the illuminated regions because the photovoltaic effect on

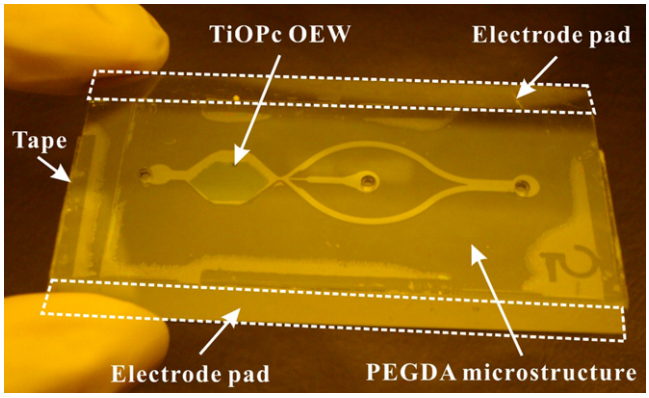

Fig. 7. The physical device of combining PEGDA-based microstructure and TiOPc-based OEW. The thickness of PEGDA microstructure is defined by tapes. Two electrode pads are used to connect the external AC bias.

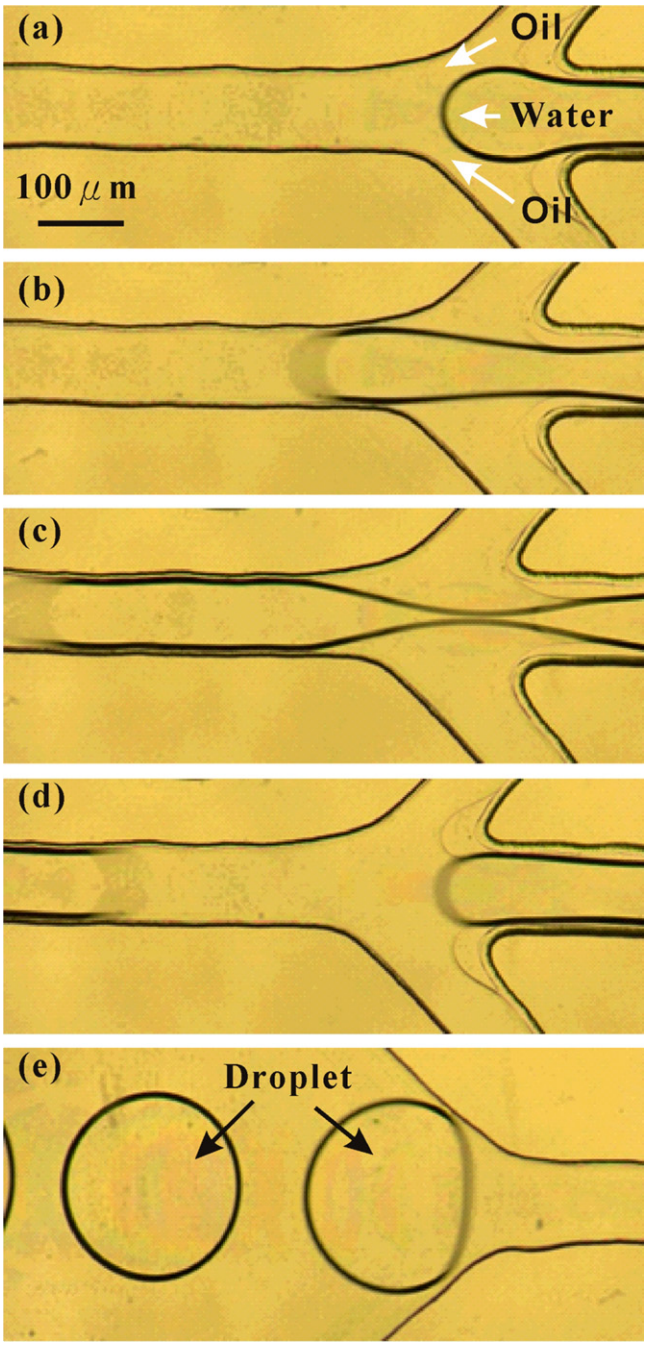

Fig. 8. Droplet generation results from the flow-focus channel junction of oil and water streams. (a)–(e) demonstrate the procedure of droplets generation in which the water stream breaks into droplets when its viscous shear overcomes its interfacial tension. The positions of (a–d) and (e) are located respectively in the droplets generation and manipulation areas.

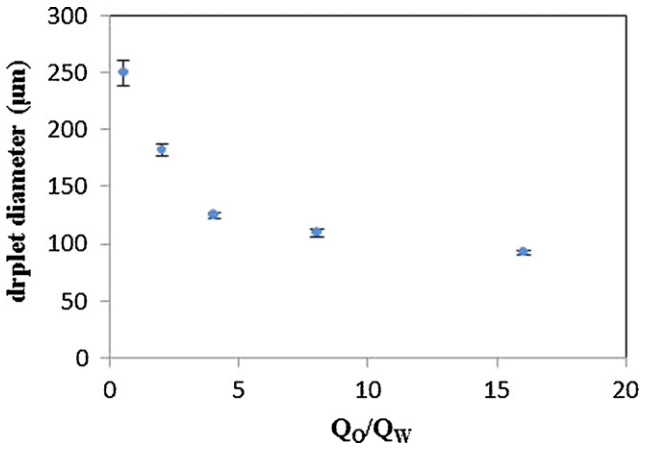

Fig. 9. The droplet diameters in different flow ratio of Q_W and Q_O.

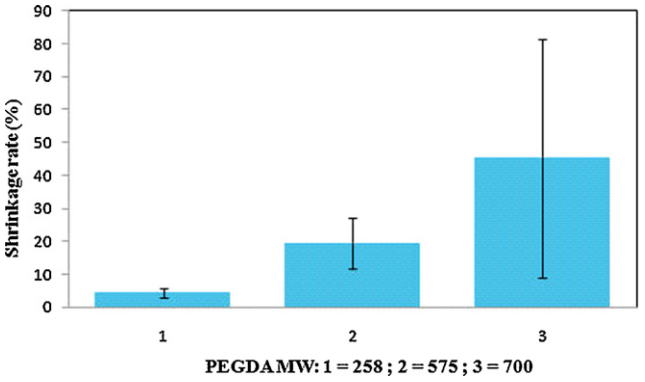

Fig. 10. The shrinkage rate of different PEGDA materials (MW 258, 575 and 700).

the illuminated TiOPc layer enhances the electrical conductivity locally. The virtual electrodes induced by optical images generate OEW effect to change contact angles of droplets resting on the surface of the dielectric (SU-8) layer.

(2) **Electrical part** provides electrical control on the frequency and amplitude of the AC bias. This part includes a function generator (33220A, Agilent Technologies, Inc., United States) and an AC voltage amplifier (High Speed Bipolar Amplifier HAS 4012 DC-1 MHz/100VA, NF Corporation, Japan) to support enough AC power for electrowetting actuation. AC signal from the function generator is amplified through the AC voltage amplifier to produce higher voltage with frequency from 10 to 100 kHz for OEW experiments. The frequency of AC signal is adjusted from low to high to find the optimal value which creates the strongest OEW effect with light illumination.

(3) **Pumping part** pumps oil and water streams into PEGDA-based microchannels for droplet generation. This part includes two syringe pumps (SP230IW SYRINGE PUMP, World Precision Instruments, Inc., United States) to respectively load water and oil into the inlets of the chip. Different sizes of droplets are formed by controlling the flow rate ratio of oil and water for droplets manipulation in the TiOPc OEW area.

4. Results and discussions

4.1. The integration of PEGDA microfluidics and TiOPc OEW

Fig. 7 shows a physical PEGDA-based microfluidic chip with TiOPc OEW inside. This device exhibits the good optical transparency and the robust packaging between the stacked ITO glass chips after the PEGDA photopolymerization. Oil (5cst, Dow Corning) and water are loaded into the inlets of PEGDA-based microfluidic chip and meet in the droplet generation area to produce monodispersed droplets (as shown in Fig. 8).

The droplet diameters in the different flow ratio of the continuous phase flow rate (Q_O, μl/min) and the dispersed phase flow rate (Q_W, μl/min) are measured in PEGDA-based microfluidic chip with

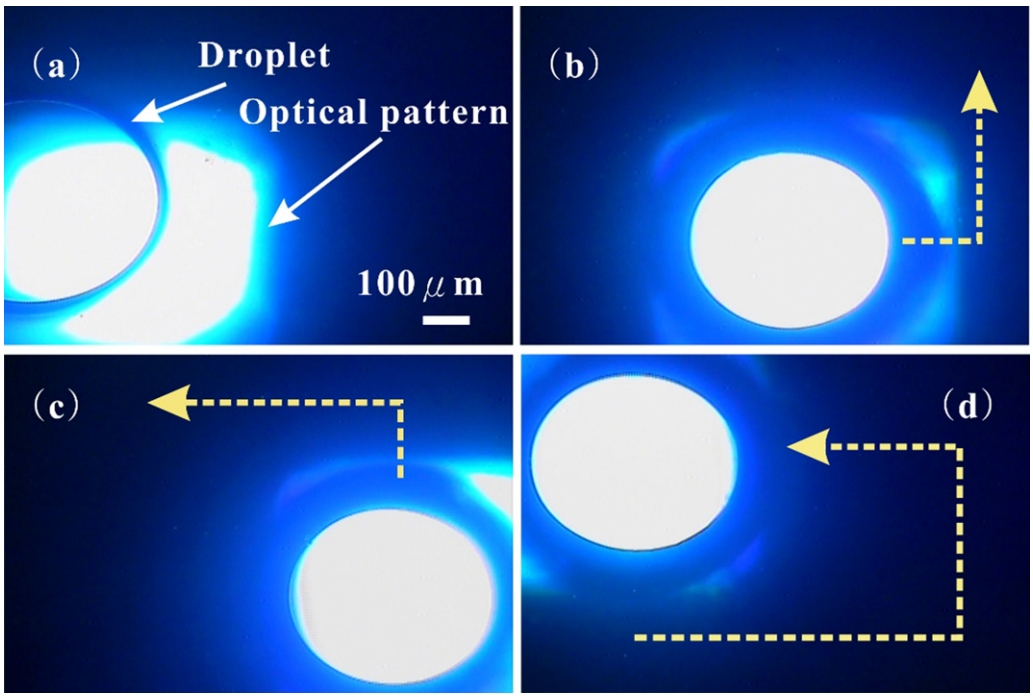

Fig. 11. Water droplet in air: (a) the droplet partially intersects with the optical rectangle pattern without AC bias. (b)–(d) After AC bias is applied, the droplet is fully overlapped and moved with the optical rectangle pattern.

the height of 40 μm tapes. The result shows the droplet diameter is reduced by increasing the flow ratio Q_O/Q_W, as shown in Fig. 9. The production of well calibrated nano-liter droplets in this microchannel dimension proved that PEGDA-based microfluidics is suitable for water droplets in oil system.

4.2. Comparison of different MW PEGDA microstructure

In traditional PEGDA microstructure for biological applications, PEGDA material shrinks after being immersed in a liquid environment. For PEGDA-based microfluidics, the stability of structure in liquid is a critical issue. We use three different molecular weight of PEGDA (MW 258, 575, 700) to fabricate the microchannel and investigate the relationship between shrinkage and molecular weight in these materials. Three molecular weight PEGDA phtocurable solutions are prepared with the same mixing ratio of PEGDA and photoinitiator (100:2). The optimized UV photopolymerization time among MW 258, 575 and 700 are 9 s, 6 s and 3 s respectively. These three MW PEGDA-based microstructure devices are immersed into water for 1 h, their shrinkage results are shown in Fig. 10. The LMW PEGDA (MW 258) with the lowest shrinkage rate among these materials can provide the stable and robust structure for microfluidic applications.

4.3. Water droplets in air with TiOPc OEW

We demonstrate the phenomenon of TiOPc OEW by controlling the motion of a water droplet in air. The solution of 0.1 M KCl is prepared as the dispersed phase flow for droplet formation. The addition of KCl can reduce the instability of droplets under the high applied voltage in electrowetting operation [11]. The Fig. 11(a) shows that an optical rectangle pattern is placed near a droplet without AC signal applied on the top and the bottom ITO glass chips. The droplet partially intersects with the optical rectangle pattern without AC bias. Fig. 11(b) shows that contact angle of the droplet touched on the bottom ITO glass decreases (as evidenced by the wider, darker ring outside the droplet) when AC signal (bias = 130 Vpp, frequency = 500 Hz) is applied. The droplet starts to move towards the inside of and become fully overlapped with the optical rectangle pattern. Fig. 11(c) and (d) shows the droplet is trapped and manipulated by the optical rectangle pattern. The measured velocity of the droplet movement is about 26 μm/s.

4.4. Water droplets in oil with TiOPc OEW

In the droplet-in-oil system, water droplets were generated and transported into the TiOPc OEW area and became ready to be manipulated by the designed optical pattern. Without illumination, the voltage drop is distributed evenly across the insulating oil medium, SU-8 and TiOPc layers. When the optical patterns are projected onto the chip, the induced virtual electrodes generate the non-uniform electrical field in the insulating oil layer and change the surface energy of the SU-8 layer. Two kinds of optoelectronic forces, OET and OEW, contribute to the motion of water droplets in the insulating oil layer. Since the water droplets are much more conductive than the surrounding electrically insulating oil, the light-induced positive DEP force drives the droplet towards the strong electric field region, the edge of the optical pattern. OEW reduces the contact angle of the droplet, which touches the virtual electrode, and traps the droplet towards the inside of the optical pattern. By adjusting the frequency of the electrical potential, we make the larger electrical impedance across the SU-8 layer than the TiOPc layer and the insulating oil medium with the light illumination [19]. The large voltage drop across the SU-8 layer enhances the electrowetting effect on the liquid droplets. The OEW effect dominates the motion of droplets over the OET effect. Our experimental results show that the OEW actuation is the dominant force because water droplets are trapped into the inside of the optical pattern during the operation.

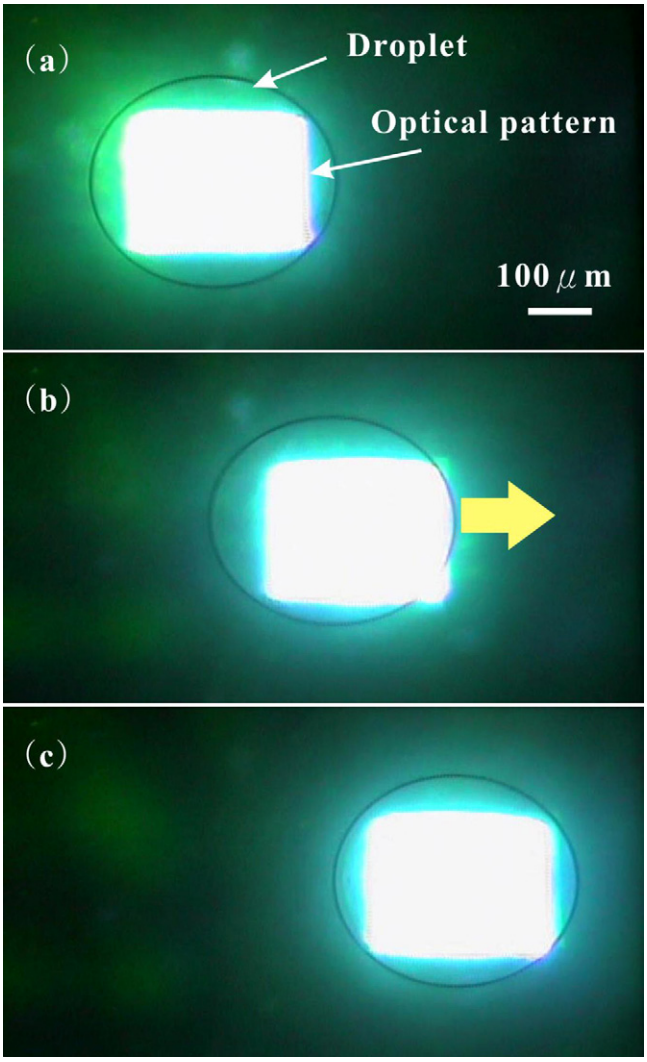

Fig. 12. Water droplet in oil: (a) the droplet is trapped by an optical pattern when AC signal is applied, (b) and (c) the droplet is driven by the movement of the optical pattern.

Fig. 12 shows that a droplet is trapped and actuated by an optical rectangle pattern in the silicone oil environment. When AC signal (bias = 188 Vpp, frequency = 500 Hz) is applied, a water droplet follows the direction of an optical pattern movement (Fig. 12(a)–(c)). The measured velocity of the droplet movement is about 39 μm/s. Comparing with water droplets in air, droplets move more smoothly in oil. The droplet manipulation is successful by TiOPc OEW at frequency range from 100 Hz to 500 Hz (at AC bias = 188 Vpp). When the frequency exceeds 800 Hz, the force produced by TiOPc OEW becomes weak and unable to control the motion of droplets.

Comparing to the droplets manipulation in the conventional (a-Si based) OEW, the lower driving speed of droplets in TiOPc-based OEW is discussed from the electrowetting theory and OEW theory by using equivalent circuit model. Based on the electrowetting theory, the lower dielectric constant and larger thickness (1 μm) of the dielectric (SU-8) layer result in the smaller change of contact angle in our TiOPc OEW than the conventional a-Si OEW. In OEW equivalent circuit model, the frequency of the electrical potential, the impedance of SU-8 and the conductivity of the photoconductor are

important factors to affect the OEW actuation. The light and dark conductivities of the TiOPc layer are not yet optimized in our OEW device. Our TiOPc OEW generates the weaker driving forces than the conventional a-Si OEW. By improving these factors, the driving speed of droplets is expected to be enhanced under the TiOPc OEW operation.

5. Conclusion

In this paper, we successfully demonstrated the integration of PEGDA-based microfluidic chip and TiOPc-based OEW by using a simpler fabrication process of spin-coating and UV photopolymerization. Stable and massive droplets are generated in the biocompatible PEGDA microstructure and dynamically manipulated by TiOPc OEW. Our TiOPc OEW in PEGDA microfluidic chip successfully trapped and moved liquid droplets both in air and oil environments. For improving the TiOPc OEW performance, the intensity of light source should be increased to enhance the conductivity of TiOPc layer and the impedance matching among insulating oil, TiOPc and SU-8 layers can be optimized for making most of the voltage drop across SU-8 layer when light illumination. In the future, other kinds of droplets, such as bubbles and culture medium solution, can be studied with our system. Customizable design of PEGDA-based microfluidics and programmable TiOPc OEW are promising in droplet manipulation steps, such as transporting, merging, mixing, and splitting, necessary for diverse bio-analytical processes.

Acknowledgments

This research was supported by the National Science Council of Taiwan, under the grant NSC-98-2120-M-007-003. The authors would like to thank Sinonar Corp. (Taiwan) for providing TiOPc material and helping the fabrication.

References

[1] C.N. Baroud, F. Gallaire, R. Dangla, Dynamics of microfluidic droplets, Lab Chip 10 (2010) 2032–2045.
[2] P. Guillot, A. Colin, Stability of parallel flows in a microchannel after a T junction, Phys. Rev. E 72 (2005) 066301.
[3] B.J. Adzima, S.S. Velankar, Pressure drops for droplet flows in microfluidic channels, J. Micromech. Microeng. 16 (2006) 1504–1510.
[4] S.L. Anna, N. Bontoux, H.A. Stone, Formation of dispersions using 'flow-focusing' in microchannels, Appl. Phys. Lett. 82 (2003) 364–366.
[5] D.R. Link, S.L. Anna, D.A. Weitz, H.A. Stone, Geometrically mediated breakup of drops in microfluidic devices, Phys. Rev. Lett. 92 (2004) 054503.
[6] A.R. Abate, A. Poitzsch, Y. Hwang, J. Lee, J. Czerwinska, D.A. Weitz, Impact of inlet channel geometry on microfluidic drop formation, Phys. Rev. E 80 (2009) 026310.
[7] M.G. Pollack, A.D. Shenderov, R.B. Fair, Electrowetting-based actuation of droplets for integrated microfluidics, Lab Chip 2 (2002) 96–101.
[8] S.K. Cho, H. Moon, C.J. Kim, Creating, transporting, cutting, and merging liquid droplets by electrowetting-based actuation for digital microfluidic circuits, J. Microelectromech. Syst. 12 (2003) 70–80.
[9] W. Satoh, H. Hosono, H. Yokomaku, K. Morimoto, S. Upadhyay, H. Suzuki, Integrated electrochemical analysis system with microfluidic and sensing functions, Sensors 8 (2008) 1111–1127.
[10] J. Zhou, L. Lua, K. Byrapogua, D.M. Woottonb, P.I. Lelkesc, R. Faird, Electrowetting-based multi-microfluidics array printing of high resolution tissue construct with embedded cells and growth factors, Virtual Phys. Prototyping 2 (2007) 217–223.
[11] F. Mugele, J.C. Baret, Electrowetting: from basics to applications, J. Phys.: Condens. Mater. 17 (2005) R705–R774.
[12] S.K. Fan, T.H. Hsieh, D.Y. Lin, General digital microfluidic platform manipulating dielectric and conductive droplets by dielectrophoresis and electrowetting, Lab Chip 9 (2009) 1236–1242.
[13] H.S. Chuang, A. Kumar, S.T. Wereley, Open optoelectrowetting droplet actuation, Phys. Rev. Lett. 93 (2008) 064104.
[14] P.Y. Chiou, H. Moon, H. Toshiyoshi, C.J. Kim, M.C. Wu, Light actuation of liquid by optoelectrowetting, Sens. Actuators A 104 (2003) 222–228.
[15] P.Y. Chiou, S. Park, M.C. Wu, Continuous optoelectrowetting for picoliter droplet manipulation, Appl. Phys. Lett. 93 (2008).
[16] S. Park, M.A. Teitell, P.Y. Chiou, Light patterned continuous electrowetting on a single photoconductive surface, Lab Chip 10 (2010) 1633–1740.
[17] S. Park, S. Kalim, C. Callahan, M. Teitell, P.Y. Chiou, A light-induced dielectrophoretic droplet manipulation platform, Lab Chip 9 (2009) 3228–3235.
[18] S. Park, C. Pan, T.H. Wu, C. Kloss, S. Kalim, C.E. Callahan, M. Teitell, E.P.Y. Chiou, Floating electrode optoelectronic tweezers: light-driven dielectrophoretic droplet manipulation in electrically insulating oil medium, Appl. Phys. Lett. 92 (2008) 151101.
[19] J.K. Valley, S. NingPe, A. Jamshidi, H.Y. Hsu, M.C. Wu, A unified platform for optoelectrowetting and optoelectronic tweezers, Lab Chip 11 (2011) 1292–1297.
[20] K.Y. Law, Organic photoconductive materials: recent trends and developments, Chem. Rev. 99 (1993) 449–485.
[21] S.M. Yang, T.M. Yu, H.P. Huang, M.Y. Ku, L. Hsu, C.H. Liu, Dynamic manipulation and patterning of microparticles and cells by using TiOPc-based optoelectronic dielectrophoresis, Opt. Lett. 35 (2010) 1959–1961.
[22] S.M. Yang, T.M. Yu, H.P. Huang, M.Y. Ku, S.Y. Tseng, C.L. Tsai, H.P. Chen, L. Hsu, C.H. Liu, Light-driven manipulation of pico-bubbles on a TiOPc-based optoelectronic chip, Appl. Phys. Lett. 98 (2011) 153512.
[23] S.M. Yang, T.M. Yu, M.H. Liu, L. Hsu, C.H. Liu, Moldless PEGDA-based optoelectrofluidic platform for microparticle selection, Adv. OptoElectron. 2011 (2011) 1–8.
[24] P.Y. Chiou, A.T. Ohta, M.C. Wu, Massively parallel manipulation of single cells and microparticles using optical images, Nature 436 (2005) 370–372.
[25] G.J. Shah, A.T. Ohta, P.Y. Chiou, M.C. Wu, C.J. Kim, EWOD-driven droplet microfluidic device integrated with optoelectronic tweezers as an automated platform for cellular isolation and analysis, Lab Chip 9 (2009) 1732–1739.
[26] S.L. Neale, M. Mazilu, J.I.B. Wilson, K. Dholakia, T.F. Krauss, The resolution of optical traps created by light Induced dielectrophoresis (LIDEP), Opt. Express 15 (2007) 12619–12626.
[27] M. Hoeb, J.O. Radler, S. Klein, M. Stutzmann, M.S. Brandt, Light-induced dielectrophoretic manipulation of DNA, Biophys. J. 93 (2007) 1032–1038.
[28] J.K. Valley, A. Jamshidi, A.T. Ohta, H.Y. Hsu, M.C. Wu, Operational regimes and physics present in optoelectronic tweezers, J. Microelectromech. Syst. 17 (2008) 342–350.
[29] H.Y. Hsu, A.T. Ohta, P.Y. Chiou, A. Jamshidi, S.L. Neale, M.C. Wu, Phototransistor-based optoelectronic tweezers for dynamic cell manipulation in cell culture media, Lab Chip 10 (2010) 165–172.
[30] J.K. Valley, S. Neale, H.Y. Hsu, A.T. Ohta, A. Jamshidi, M.C. Wu, Parallel single-cell light-induced electroporation and dielectrophoretic manipulation, Lab Chip 9 (2009) 1714–1720.
[31] A.M. Kloxin, A.M. Kasko, C.N. Salinas, K.S. Anseth, Photodegradable hydrogels for dynamic tuning of physical and chemical properties, Science 324 (2009) 59–63.
[32] G.B. Schneider, A. English, M. Abraham, R. Zaharias, C. Stanford, J. Keller, The effect of hydrogel charge density on cell attachment, Biomaterials 25 (2004) 3023–3028.
[33] J. Yeh, Y. Ling, J.M. Karp, J. Gantz, A. Chandawarkar, G. Eng, J. Blumling III, R. Langer, A. Khademhosseini, Micromolding of shape-controlled, harvestable cell-laden hydrogels, Biomaterials 27 (2006) 5391–5398.
[34] M.P. Cuchiara, A.C.B. Allen, T.M. Chen, J.S. Miller, J.L. West, Multilayer microfluidic PEGDA hydrogels, Biomaterials 31 (2010) 5491–5497.
[35] C.M. Nelson, W.F. Liu, C.S. Chen, Control of mammalian cell and bacteria adhesion on substrates micropatterned with poly(ethylene glycol) hydrogels, Biomed. Microdevices 5 (2003) 11–19.
[36] D.R. Albrecht, V.L. Tsang, R.L. Saha, S.N. Bhatia, Photo- and electropatterning of hydrogel-encapsulated living cell arrays, Lab Chip 5 (2005) 111–118.
[37] C.M. Hwang, W.Y. Sim, S.H. Lee, A.M. Foudeh, H. Bae, S.H. Lee, A. Khademhosseini, Benchtop fabrication of PDMS microstructures by an unconventional photolithographic method, Bio-fabrication 2 (2010) 045001.

Biographies

Tung-Ming Yu received the M.S. degree in Electrophysics from Chiao-Tung University, Taiwan, in 2002. He was an engineer responsible for developing the microfluidic chips for the biological diagnosis applications and medical electronic devices for homecare use in Industrial Technology Research Institute (ITRI), Taiwan, for 7 years. He is currently a Ph.D. candidate in the Department of Electrophysics at Chiao-Tung University, Taiwan. His research interests include laser tweezers, dielecphoresis, optoelectronic tweezers and opto-electrowetting.

Shih-Mo Yang received a B.S. degree in physics from National Changhua University of Education, in 2000, and the M.S. degree in physics from National Tsing Hua University, Taiwan, in 2004. After four years being a physics teacher for senior high school. He is currently a Ph.D. candidate in the Electrophysics Department, National Chiao-Tung University, Taiwan. His research interests are in liver lab chip, tissue engineering, BioMEMS, microfluidics design and optoelectronics system for biomedicine applications.

Chien-Yu Fu is currently a PhD student at the Institute of Molecular Medicine, National Tsing Hua University (NTHU), Hsinchu, Taiwan. She is interested in applying microfluidic systems in biomedical research and tissue engineering.

Ming-Huei Liu received his Ph.D. in Chemical Engineering from the National Cheng-Kung University in 1997 and joined Sinonar Corp. in 2001. Previously at R&D department in Sinonar his work focused primarily on the development of organic

photoconductors for color electrophotography. Currently, his work is mainly in the development of chemically produced toners for color electrophotography.

Long Hsu received his Ph.D. degree in physics from Massachusetts Institute of Technology, USA. He was a postdoctoral researcher in College of Medicine, University of California, San Francisco. He is currently a associate professor in the Electrophysics Department at National Chiao-Tung University, Taiwan. His research expertise include semiconductor laser, laser tweezers, gene wafer, nano photonic-bio Technology.

Hwan-You Chang is currently a professor at the Institute of Molecular Medicine, National Tsing Hua University (NTHU), Hsinchu, Taiwan. He received his PhD in Basic Medical Sciences from the New York University in 1988. He then undertook postdoctoral research in the Dana-Farber Cancer Institute in Boston between 1988 and 1989. He then moved to Chang Gung University, Taiwan and became an associate professor in May 1989. He was recruited to NTHU in August 1997. He is interested in applying microelectromechanical systems and nanotechnology in biomedical research.

Cheng-Hsien Liu received his Ph.D. degree in mechanical engineering from Stanford University. Presently he is a professor in the Power Mechanical Engineering Department at National Tsing Hua University. His research activities cover a variety of areas in MicroElectroMechanical Systems, System Dynamics/Modeling/Control and Nanotechnology. He received A. Kobayashi Young Investigator Award in Experimental Science from International Conference on Computational and Experimental Engineering and Sciences in 2000, the award of Outstanding Chemical Engineering Article of the Year 2010, the award for University Special Talents from National Science Council (2010–2011), the Academic Excellent Award from National Tsing Hua University.